Journal of Power Sources 224 (2013) 317–323

Contents lists available at SciVerse ScienceDirect

Journal of Power Sources

journal homepage: www.elsevier.com/locate/jpowsour

Preparation and capacitive properties of the core–shell structure carbon aerogel microbeads- nanowhisker-like NiO composites

Xingyan Wang [a,b,**], Xianyou Wang [b,*], Lanhua Yi [b], Li Liu [b], Youzhi Dai [a,b], Hao Wu [b]

[a] College of Chemical Engineering, Xiangtan University, Xiangtan 411105, China
[b] Key Laboratory of Environmentally Friendly Chemistry and Applications of Ministry of Education, Xiangtan University, Hunan, Xiangtan 411105, China

HIGHLIGHTS

- NiO/CAMB composite materials with core–shell structure were prepared.
- The optimum amount of NiO in NiO/CAMB composite is 15 wt.%.
- Coating NiO on the CAMB could improve the supercapacitive behaviors of composites.

ARTICLE INFO

Article history:
Received 14 August 2012
Received in revised form
15 September 2012
Accepted 17 September 2012
Available online 5 October 2012

Keywords:
Carbon aerogel microbeads
Nickel oxide
Core–shell structure
Supercapacitor
Electrochemical performance

ABSTRACT

In current study, nanowhisker-like NiO/carbon aerogel microbead (NiO/CAMB) composites with chestnut-like core–shell structure are prepared by in situ encapsulating method. The structure and morphology of NiO/CAMB are characterized by X-ray diffraction (XRD), scanning electron microscopy (SEM) and transmission electron microscopy (TEM). Results indicate that the appearance of composite becomes chestnut-like morphology with core–shell structure when NiO is coated. Electrochemical performances of the NiO/CAMB composites with different NiO contents are evaluated by using cyclic voltammetry (CV), galvanostatic charge–discharge and electrochemical impedance spectroscopy (EIS). Results show that the supercapacitive behaviors of NiO/CAMB composites are largely improved due to the combination of electrical double-layer capacitance of CAMB and pseudo-capacitance based on the redox reaction of NiO. Especially, the 15%-NiO/CAMB composite exhibits the best capacitive properties, its specific capacitance is up to 356.2 F g^{-1}. Besides, the symmetric supercapacitor using 15%-NiO/CAMB composite as the electrode active material shows stable cycling performance.

1. Introduction

In the energy storage research field, supercapacitors are also known as electrochemical capacitors. Compared with traditional batteries, they are essentially maintenance-free, possess a longer cycle life, require a very simple charging circuit, experience no memory effect, and are generally much safer [1]. They are particularly adapted for applications which require energy pulses during short periods of time [2,3]. One of the most promising supercapacitor applications is in electric vehicles. Supercapacitors can be coupled with fuel cells or batteries to deliver the high power needed during acceleration and to recover the energy during braking [4]. On the mechanisms of charge storage, supercapacitors are generally classified as: (a) electrical double-layer capacitors (EDLCs) that employ carbon or other similar materials as electrodes, and (b) redox supercapacitors, which are based on the pseudo-capacitance arising from fast and reversible faradic redox reactions of electroactive materials [5]. The carbon-based double layer capacitors usually exhibit good stability, but limited EDLC capacitance [6]. Transition-metal oxides produce pseudo-capacitance through the multielectron transfer during the fast faradic reaction. However, the metal oxides suffer from drawbacks of low electrical conductivity, high cost, and poor cycling stability [7,8]. Although the conducting polymers have shown high pseudo-capacitance, poor cyclic stability hinders their commercial application [9]. Therefore, pure carbon materials, metal oxides or conducting polymers can't well meet the practical requirement for large-scale application of supercapacitors.

* Corresponding author. Tel.: +86 731 58292060; fax: +86 731 58292061.
** Corresponding author. College of Chemical Engineering, Xiangtan University, Xiangtan 411105, China.
E-mail addresses: wqinyan801@yahoo.com.cn (X. Wang), wxianyou@yahoo.com (X. Wang).

0378-7753/$ – see front matter © 2012 Elsevier B.V. All rights reserved.
http://dx.doi.org/10.1016/j.jpowsour.2012.09.064

Usually, the specific capacitance of carbon material can be improved by introducing pseudo-capacitive species on the electrode materials. The electrical conductivity and stability of transition-metal oxides can be enhanced by using a carbon support [10]. Therefore; many approaches have been employed to prepare carbon/metal oxide composites. Various metal oxides are typically active species for producing pseudo-capacitance, such as RuO_x, MnO_2, and NiO_x [11–13]. Among these materials, nickel oxide has become one of the most promising electrode materials for pseudocapacitors because of its abundance in natural, low cost, and environment compatibility [14]. However, issues related to its electrochemical characteristics, such as conductivity and the utilization of the active material, still remain unresolved. In order to further improve its performance, nickel-based compound/carbon composites are one of the most commonly used candidates for electrochemical capacitors [15], such as NiO/activated carbon and NiO/carbon nanotube [16,17].

Although some related works have been carried out on NiO/C composites in application of supercapacitor, there are fewer reports on synthesizing NiO/CAMB in situ coating method. In our previous work, CAMB was prepared and its supercapacitive performance was studied [18,19]. In this work, CAMB was applied as the substrate of NiO growth by in situ pyrogenation of nickel (II) nitrate. It was found that nanowhisker-like NiO could be homogeneously coated on the surface of CAMB to form the chestnut-like NiO/CAMB composite with core–shell structure. The capacitive properties of composites were investigated by CV, galvanostatic charge–discharge and EIS. The NiO/CAMB composite electrode showed significantly improved specific capacitance and excellent cyclic stability.

2. Experimental

2.1. Materials

All the materials and chemical reagents were of analytical grade, which were obtained from commercial sources and directly used without any pretreatment. Resorcinol, sodium carbonate, nickel (II) nitrate ($Ni(NO_3)_2 \cdot 6H_2O$) and potassium hydroxide were purchased from Guangdong Guanghua Chemical Factory Co., Ltd., China. Formaldehyde and acetone were obtained from Changsha Antai Fine Chemical Co., Ltd., China. Hexamethylene and SPAN 80 were provided by Institute of Guangfu Fine Chemical, Tianjin, China. Double distilled water of 18 MΩ cm was used to prepare the solutions.

2.2. Preparation of NiO/CAMB composites

CAMB was synthesized by an inverse emulsion polymerization of resorcinol with formaldehyde. The detailed procedure was reported in our previous work [19]. The typical preparation procedure for NiO/CAMB composite was as follows: proper amount of nickel nitrate was dissolved in distilled water, and the solution was then added dropwise onto the CAMB, the mixture was magnetically stirred for 4 h in room temperature to assure that $Ni(NO_3)_2$ was fully adsorbed on the surface of CAMB. The amount of NiO was set at 5, 10, 15 and 20 wt.%. The resultant mixture was dried at 353 K for 12 h, and subsequently, it was calcined at 623 K for 5 h under Ar atmosphere. The NiO/CAMB composite was obtained finally. The name of NiO/CAMB composite material was abbreviated as *x*-NiO/CAMB, where *x* delegates the content of NiO in the composite. For example, 10 wt.% NiO was called 10%-NiO/CAMB. In comparison, the pure NiO was prepared by calcining nickel nitrate at 623 K.

2.3. Characterization of structure and morphology

(1) X-ray diffraction (XRD) patterns of the samples were performed on a diffractometer (D/MAX-3C) with Cu Kα radiation (λ = 1.54056 Å) and a graphite monochromator at 50 kV, 100 mA.
(2) The morphology and surface structure of the samples were investigated with a scanning electron microscopy (SEM) (JSM-6610, JEOL) and a transmission election microscope (TEM, FEI Tecnai G2)

2.4. Evaluation of electrochemical properties

The mixture containing 80 wt.% active material, 10 wt.% graphite, and 10 wt.% polytetrafluoroethylene (PTFE) (60%) was well mixed in *N*-methyl-2-pyrrolidone (NMP) until to form the slurry with proper viscosity, and then the slurry was uniformly coated on a disk-like Ni foam served as a current collector and dried at 353 K for 12 h, and then pressed at 15 MPa for 1 min in order to assure a good electronic contact. The mass load of active material was 5 mg cm^{-2} and the geometric area of composite electrodes is 1 cm^2. Electrochemical performances of the electrodes were characterized by cyclic voltammetry (CV), electrochemical impedance spectroscopy (EIS) in the frequency range of 1×10^5 to 1×10^{-2} Hz and galvanostatic charge–discharge tests in 6 M KOH. The CV and EIS tests were performed by electrochemical analyzer systems (CHI660A) with three-electrode system, in which the Ni foam and the Hg/HgO electrode were used as counter and reference electrodes, respectively. The galvanostatic charge–discharge and cycle life tests were carried out by potentiostat/galvanostat (BTS6.0, Neware, Guangdong, China) on button cell supercapacitors. The symmetrical button cell supercapacitors were assembled according to the order of electrode–separator–electrode.

3. Results and discussion

3.1. Material characterization

The X-ray diffraction patterns of the composites with different NiO content are shown in Fig. 1. The XRD pattern of pure CAMB shows two broad diffraction peaks at $2\theta \approx 24°$ and 44°, corresponding to (002) and (101) diffraction peaks of graphitic carbon,

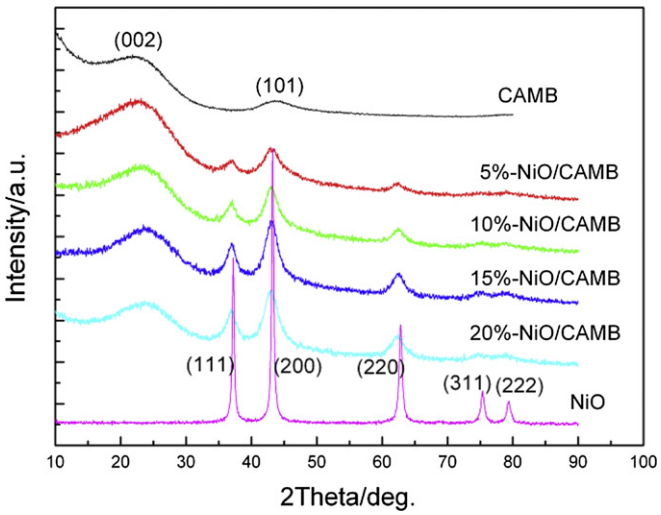

Fig. 1. XRD patterns of CAMB and NiO/CAMB composites.

and thus CAMB is slightly graphitized and has enhanced electrical conductivity [16]. The diffraction peaks of NiO appeared at 37.19°, 43.23°, 62.81°, 75.33°, and 79.31° are in good agreement with the (111), (200), (220), (311), and (222) planes of face-centered cubic (fcc) NiO (JCPDS card no. 73-1523). The XRD patterns of NiO/CAMB composites show both characteristic features of CAMB and NiO. The diffraction peaks of NiO in composites become broader due to the presence of CAMB support. It can also be seen from Fig. 1 that the NiO in the as-prepared NiO/CAMB composite shows less-developed crystallization than pure NiO, which is more suitable for supercapacitor electrode material, because the amorphous structure is conducive to the infiltration for electrolyte than the crystal structure [20].

The SEM images of CAMBs and NiO/CAMB composites with different amount of NiO are shown in Fig. 2. The as-prepared CAMB shows perfectly spherical shape (Fig. 2a), in our previous work [19], it has proved that the CAMB is a typical mesoporous carbon material and the average pore size is around 4.95 nm in the range of mesopore (between 2 and 50 nm), which ensure the access of electrolyte into the electrode material and will result in a higher double-layer capacitance. For composite, the original spherical shape of CAMB is still retained during the coating process, but the surface morphologies of NiO/CAMB composites change when NiO is coated. Furthermore, it has been noted that the morphologies of the composites are closely related to the amount of NiO on the surface of CAMB. For 5%-NiO/CAMB composite sample, the NiO particles are randomly distributed on the surface of CAMB (Fig. 2b) and can't homogeneously encapsulate the whole spherical particle. In the case of 10%-NiO/CAMB, a layer of flocculent deposits are coated on the surface of spherical CAMB particle (Fig. 2c); however the deposits are not completely coated on the whole surface of CAMB. Fig. 2d and f shows that 15 wt.% NiO can be more evenly dispersed on the surface of spherical CAMB particle and form a uniform chestnut-like core–shell structure with CAMB as the core and NiO as the shell. From the high magnification SEM image (Fig. 2f), whisker-like NiO nanoparticles can be seen on the surfaces of CAMB. Compared with 15%-NiO/CAMB sample, when the amount of NiO is 20 wt.%, the size of NiO nanoparticles and thickness of the NiO shell increase apparently.

In order to further analyze the morphology of NiO, the TEM micrographs of 15%-NiO/CAMB are shown in Fig. 3. It can be found that the whisker-like NiO nanofibre is about 60–80 nm in diameter and 300 nm in length. The presence of nanowhisker-like NiO shell can provide high Faradic capacitance, and the presence of CAMB

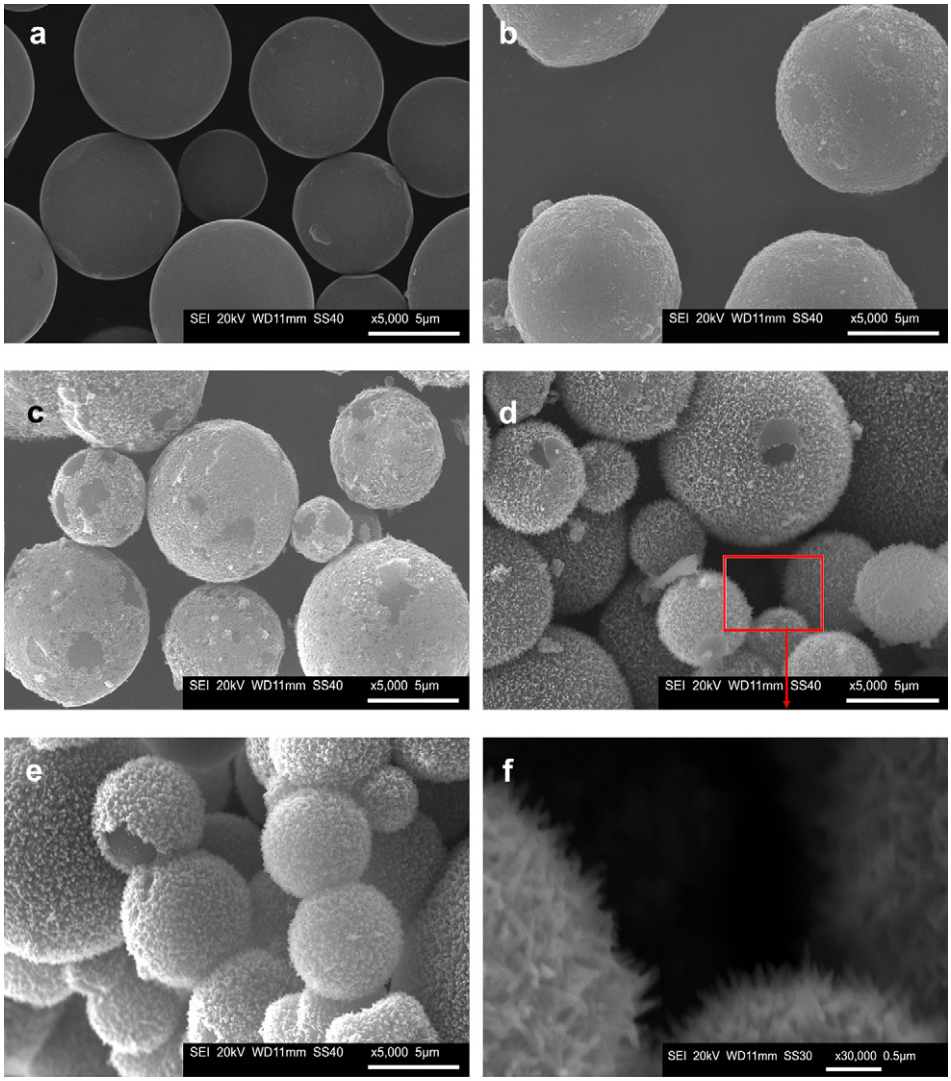

Fig. 2. SEM images of the samples: (a) CAMB, (b) 5%-NiO/CAMB, (c) 10%-NiO/CAMB, (d) 15%-NiO/CAMB, (e) 20%-NiO/CAMB; (f) The SEM image of 15%-NiO/CAMB at higher magnification.

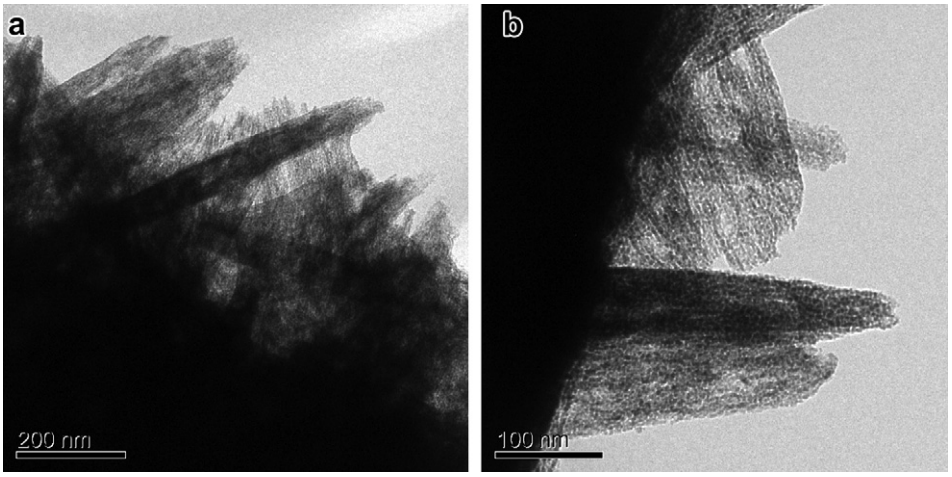

Fig. 3. TEM images of 15%-NiO/CAMB.

core can improve the electronic conductivity and produce electric double layer capacitance. Thus it can be expected that the NiO/CAMB composite would provide an improved electrochemical performance.

3.2. Electrochemical characterization

Supercapacitive behavior of material can be evaluated through three-electrode test and double-electrode test (symmetric supercapacitors). Generally, three-electrode system is used to qualitative analysis or semi-quantitative analysis, such as the reversibility and mechanism of electrochemical reaction. Usually, choosing the appropriate potential window, the specific capacitance of single electrode ($C_{s.t}$) can be measured by CV test with three-electrode system. Besides, the specific capacitance (C_m) and cyclic stability of capacitor can be measured by two-electrode system. In this work, two-electrode system is equal to a symmetric capacitor, which is comprised of two equivalent capacitors (single electrode capacitor) in series. Total capacitance of capacitor C_{total} is contributed by both positive (C_+) and negative (C_-) electrodes and can be calculated by the equation below [21]:

$$\frac{1}{C_{total}} = \frac{1}{C_+} + \frac{1}{C_-} \tag{1}$$

For symmetric capacitor, $C_+ = C_- = C$,

$$C_{total} = \frac{C}{2} \tag{2}$$

$$C_{s.t} = \frac{C}{m} \quad C_m = \frac{C_{total}}{2m} \tag{3}$$

where C_{total} is the values of total capacitance of the two-electrode cell (F),

C is the capacitance of the single electrode (F),

m is the mass of active material on electrode (g),

$C_{s.t}$ is the specific capacitance of the electrode (F g^{-1}),

C_m is the specific capacitance of capacitor (F g^{-1}).

It should be noted that the factor two for series capacitance and factor two for double weight of single electrode have been taken into account, so $C_{s.t}$ should be four times of C_m in theory [22].

The CV curves of CAMB and NiO/CAMB composites are shown in Fig. 4. As shown in Fig. 4, the CV of pristine CAMB exhibits a quasi-rectangular shape, implying that its capacitance is mainly contributed from the charge accumulation at the electrode/electrolyte interface. In contrast, a pair of redox peaks is observed clearly on each CV curve of NiO/CAMB composite. In spite of the change of NiO/CAMB ratios, the capacitances of NiO/CAMB composites all show combination of electrical double-layer capacitance (CAMB) and pseudo-capacitance from the redox reaction of NiO. Furthermore, it is apparent that the NiO/CAMB composite electrodes possess larger areas surrounded by CV curves. It is well-known that the capacitance of carbon double-layer capacitor is based on the charges adsorbed on the electrode/electrolyte interface; the CV curve of CAMB is close to an ideal rectangular shape. However, CV curves of NiO/CAMB composites are different from that of CAMB due to a Faradic reaction of NiO as follows [23]:

$$NiO + OH^- \Leftrightarrow NiOOH + e^- \tag{4}$$

To analyze the variation of capacitance with the NiO content and scan rate, the CV measurement was carried out, and the specific capacitance of the electrode can be calculated by Eq. (5) [24] based on CV results.

$$C \equiv \frac{Q}{V} = \int \frac{i dt}{\Delta V} \tag{5}$$

where i is a sampled current, dt is a sampling time span, and ΔV is the total potential deviation of the voltage window. Fig. 5 shows the specific capacitance variations of different NiO contents in NiO/

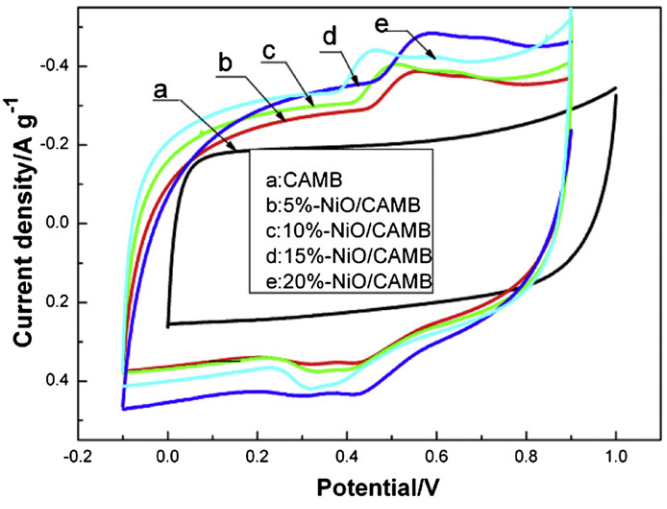

Fig. 4. Cyclic voltammograms of the samples at scan rate of 1 mV s^{-1}.

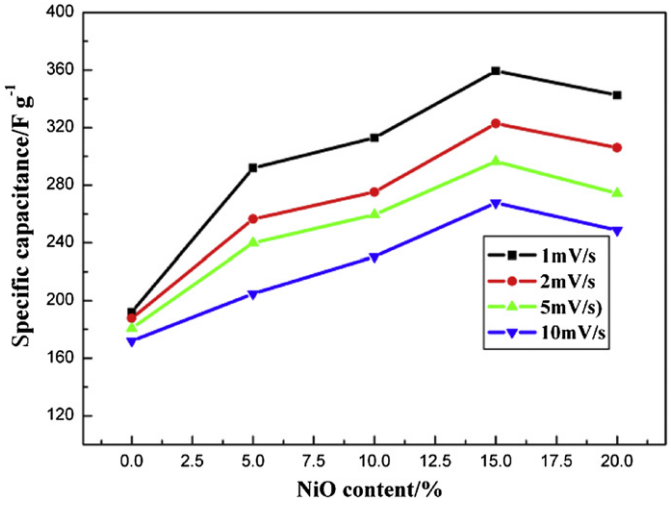

Fig. 5. Specific capacitances of electrodes with different NiO content at various scan rates.

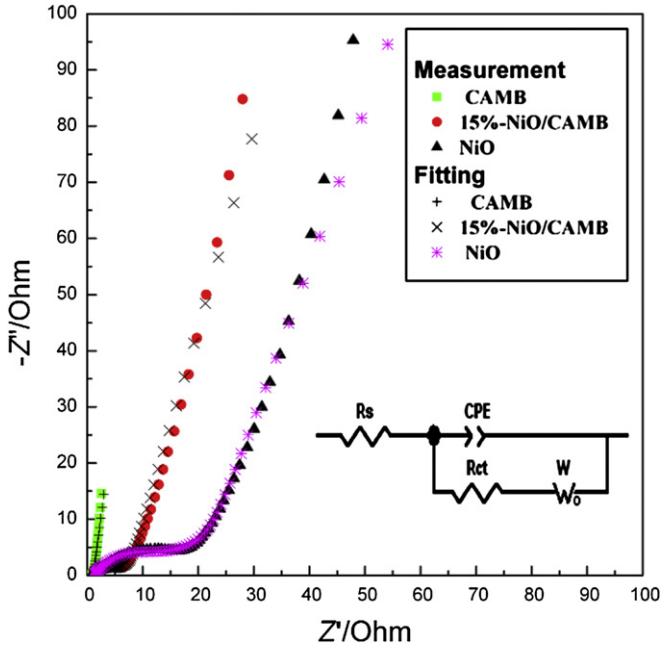

Fig. 6. Experimental and fitted impedance spectra for different electrodes.

CAMB composites with scan rate from 1 mV s^{-1} to 10 mV s^{-1}. The results suggest that the capacitance of composite is apparently improved by coating NiO on the surface of CAMB. A maximum specific capacitance of 359.4 F g^{-1} is obtained when the content of NiO is 15 wt.% at a scan rate of 1 mV s^{-1}, which is much higher than the ones of CAMB. As NiO content is higher than 15 wt.%, the specific capacitance of composite material decreases gradually. The reason is probably because the carbon surface is covered with excess amount of NiO, and it will result in the decrease of specific surface area of CAMB. This can be attributed to the loss of double-layer capacitance of carbon. As shown in Figs. 4 and 5, impregnation of certain amount of NiO can significantly improve the capacitance of CAMB and the optimum NiO content is 15 wt.%.

Electrical conduction and ion transfer were investigated by EIS analysis. Fig. 6 shows Nyquist impedance spectra for different electrodes. The impedance plots are fitted using the equivalent circuit model (an inset in Fig. 6), and the fitted values are listed in Table 1. The equivalent circuit model includes the internal resistances of the electrode materials (R_s), a constant phase element (CPE) associated with the interfacial resistance, charge transfer resistance R_{ct}, and the Warburg impedance (Z_w) that is related to the diffusion of ions in the solid oxide matrix. It should be noted that the impedance behavior of pure CAMB approaches to pure capacitive behavior, which is a straight line nearly parallel to the imaginary axis. The impedance spectra for NiO and NiO/CAMB capacitors show a small semicircle in higher frequency range followed by a straight line with a certain slope in lower frequency range. As summarized in Table 1, CAMB has the least R_s and R_{ct}, showing high electrical conductivity, however pure NiO shows poor conductivity. The resistance of 15%-NiO/CAMB increases comparing to CAMB, but the R_{ct} of 15%-NiO/CAMB composite electrode is 3.52 Ω, which is much smaller than that of NiO electrode (12.55 Ω). Therefore, coating a certain amount of NiO on the surface of CAMB can take full advantages of the high conductivity of CAMB and high capacitance of NiO.

To evaluate the electrochemical capacitance of NiO/CAMB composites, symmetrical button cell supercapacitors were assembled and characterized with galvanostatic charge–discharge measurements. The charge/discharge curves of the composite capacitors with different NiO content at a current of 1 A g^{-1} are given in Fig. 7. It can be found that the voltage of CAMB electrode varies linearly with time during charge/discharge process, and the curve is close to an isosceles triangle, which indicates ideal double-layer capacitive behavior. However, the charge/discharge curves of NiO/CAMB composite electrodes deviate from ideal linear line due to the existence of Faradaic reaction. Thus NiO/CAMB composite electrode will have much longer charge/discharge duration and much higher charge storage capacity than CAMB electrode. The average specific capacitance of composite electrode can be calculated on the basis of Eq. (6) [25]:

$$C_{s.t} = \frac{2I \times t}{\Delta V \times m} \tag{6}$$

where C_m is the specific capacitance of the electrode (F g^{-1}), m is the mass of active material in one electrode (g), I is charge/discharge current (A), t is the discharge time (s), and ΔV is the range of the charge/discharge (V). The factor of 2 comes from the fact that the total capacitance measured from the test cells in the sum of two equivalent single electrode capacitors in series. Table 2 tabulates the specific capacitances of CAMB and NiO/CAMB composite with different NiO content, which are calculated according to Eq. (6) based on charge/discharge measurements. It can be seen from Fig. 6 and Table 2 that the discharge time and the specific capacitance of 15%-NiO/CAMB are maximum, which are well consistent with the results measured by cyclic voltammetry. When NiO content is higher than 15 wt.%, the specific capacitance of the composite decreases. Because the size of NiO nanoparticles and the thickness of the NiO shell increase with the increase of NiO amount, which will result in the increase of the resistance of electrode and hamper the fast penetration of electrolyte ion.

Table 1
Values of equivalent circuit parameters for different electrodes.

Electrode	R_s/Ω	R_{ct}/Ω
CAMB	0.71	0.56
NiO	1.33	12.55
15%-NiO/CAMB	1.23	3.52

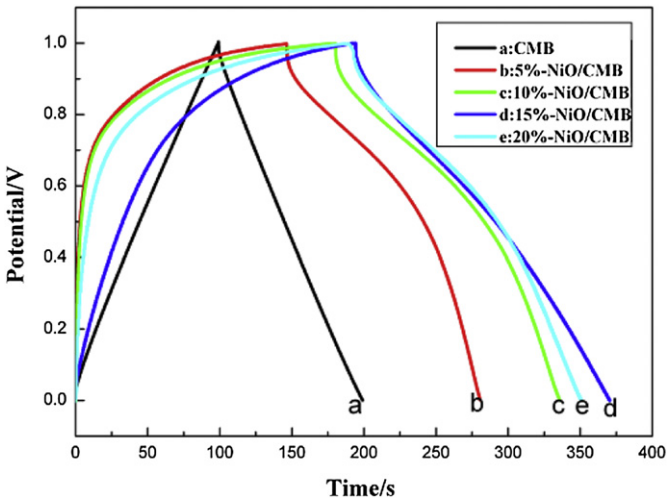

Fig. 7. Charge/discharge curves of electrodes with different NiO content in 6 M KOH electrolyte at a current of 1 A g^{-1}.

Table 2
Specific capacitance of NiO/CAMB electrodes with different NiO content at a current of 1 A g^{-1}.

NiO content (wt.%)	0	5	10	15	20
$C_{s,t}$ (F g^{-1})	196.7	273.2	311.5	356.2	316.8

Fig. 8 presents the galvanostatic charge/discharge curves of 15%-NiO/CAMB composite electrode at different current densities. The shape of the charge/discharge curves reveals the combination of double layer capacitance (CAMB) and Faradaic pseudo-capacitance (NiO). A curving variation of the potential dependence of the time was attributable to the pseudo-capacitive behavior of NiO. The specific capacitances of 15%-NiO/CAMB composite calculated from the galvanostatic discharge curves at different current density are summarized in Table 3, the specific capacitance of CAMB has tiny decrease with the increase of discharge current density, and thus an excellent rate capability can be noted. However, the specific capacitance of the NiO/CAMB composite electrodes decreases faster than that of CAMB electrode, the same phenomenon has been observed when the scan rate is increased. The main reason for such

Table 3
Specific capacitance of CAMB and 15%-NiO/CAMB electrodes at different current density.

Sample	Specific capacitance (F g^{-1})				
	1 A g^{-1}	2 A g^{-1}	3 A g^{-1}	4 A g^{-1}	5 A g^{-1}
CAMB	196.7	183.9	176.2	160.0	137.1
15%-NiO/CAMB	356.2	284.9	235.2	209.3	191.5

a behavior can be explained based on faradic reaction of NiO during the charge/discharge process. The presence of inner active sites can't precede the redox transitions completely at higher scan rates or higher discharge current density. The decreasing trend of the capacitance suggests that the parts of the inner of electrode are inaccessible at high charge/discharge rate. Hence, the specific capacitance obtained at the slowest scan rate is close to that of full utilization of the electrode material. All though the specific capacitance of 15%-NiO/CAMB composite electrode decreases faster with increasing current density, but the specific capacitance is obviously higher than that of CAMB at every given current density. Especially, the specific capacitance is up to 356.2 F g^{-1} at a current of 1 A g^{-1}, which is much higher than that of pure CAMB (196.7 F g^{-1}) and other carbon materials [26,27].

The stability and reversibility of an electrode material will be important for determining its application of supercapacitor. Symmetrical supercapacitors were assembled using CAMB and 15%-NiO/CAMB as electrode active materials, respectively. The stability of the supercapacitor was examined by repeated charge/discharge cycling between 0 and 1.0 V on symmetric capacitor. The variations of the discharge capacitance with cycle number are illustrated in Fig. 9. Although the CAMB supercapacitor exhibits excellent cycling stability and the specific capacitance maintains at a stable value till 4000 cycles, the specific capacitance is clearly lower than that of 15%-NiO/CAMB composite. Interestingly, the specific capacitance of 15%-NiO/CAMB supercapacitor shows a slight increase at the beginning of cycles, which is possibly due to the activation process of the NiO electrodes [23,28]. Thereafter, the specific capacitance of the 15%-NiO/CAMB supercapacitor is maintained at a stable value as the charge/discharge process continues, which confirms the stable cycling performance of the composite. Therefore, the poor cyclic stability of metal oxide materials in application of supercapacitor is markedly improved through using CAMB as the substrate.

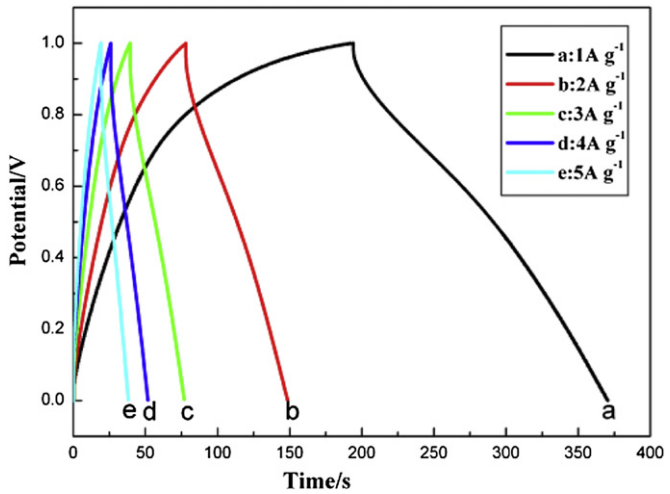

Fig. 8. Charge/discharge curves of 15%-NiO/CAMB electrode at different current densities.

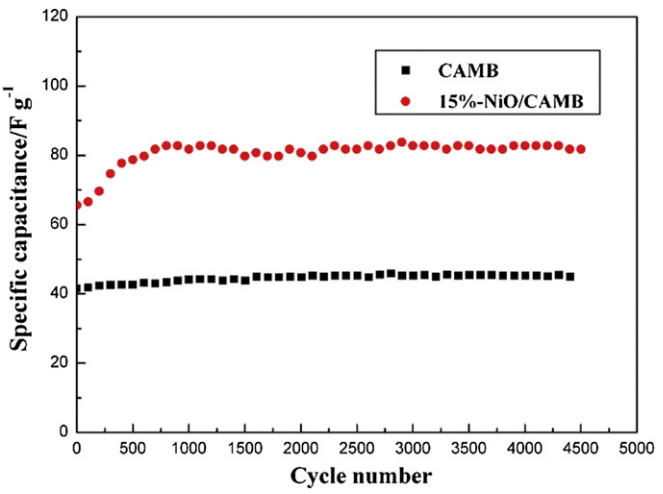

Fig. 9. Cycle life curves of supercapacitors with different active material at a current of 1 A g^{-1}.

4. Conclusions

Chestnut-like NiO/CAMB composite materials with core–shell structure for supercapacitor were successfully prepared by in situ coating method. Nanowhisker-like NiO particles were coated on the surface of CAMB and became a chestnut-like appearance. The amount of NiO apparently affects the electrochemical performance of the composites. It has been found that the optimum NiO content in composite is 15 wt.%. The specific capacitance of the 15%-NiO/CAMB composite electrode is up to 356.2 F g^{-1}, which is the combination of electrical double-layer capacitance of CAMB and pseudo-capacitance based on the redox reaction of NiO. Moreover, 15%-NiO/CAMB composite supercapacitor shows long cycle life and high rate capability. Therefore, coated NiO is an effective path for increasing specific capacitance of carbon materials for the application of supercapacitors.

Acknowledgments

This work was financially supported by the National Natural Science Foundation of China (Grant Nos. 51272221, 51072173 and 21203161), Specialized Research Fund for the Doctoral Program of Higher Education (Grant No. 20094301110005), Project supported by Science and Technology Department of Hunan Province (Grant No. 2012FJ4095), Project supported by the National Science Foundation for Post-doctoral Scientists of China (Grant No. 2012M511739), the Scientific Research Fund of Hunan Provincial Education Department (Grant No. 1200395) and Project supported by the Xiangtan University (Grant No. 2011XZX10).

References

[1] X.Y. Zhang, X.Y. Wang, L.L. Jiang, H. Wu, C. Wu, J.C. Su, J. Power Sources 216 (2012) 290–296.
[2] X.Y. Zhang, X.Y. Wang, J.C. Su, X.Y. Wang, L.L. Jiang, H. Wu, C. Wu, J. Power Sources 199 (2012) 402–408.
[3] Y.G. Wang, H.Q. Li, Y.Y. Xia, Adv. Mater. 18 (2006) 2619–2623.
[4] C.G. Liu, Z.N. Yu, D. Neff, A. Zhamu, B.Z. Jang, Nano. Lett. 10 (2010) 4863–4868.
[5] A. Malak-Polaczyk, C. Vix-Guterl, E. Frackowiak, Energy Fuels 24 (2010) 3346–3351.
[6] H. Tamai, M. Hakoda, T. Shiono, H. Yasuda, J. Mater. Sci. 42 (2007) 1293–1298.
[7] D.Y. Liu, J.R. Reynolds, ACS Appl. Mater. Interface 2 (2010) 3586–3593.
[8] A.L.M. Reddy, M. Shaijumon, M.S.R. Gowda, P.M. Ajayan, J. Phys. Chem. C 114 (2010) 658–663.
[9] L.X. Li, H.H. Song, Q.C. Zhang, J.Y. Yao, X.H. Chen, J. Power Sources 187 (2009) 268–274.
[10] J.M. Ko, K.S. Ryu, S. Kim, K.M. Kim, J. Appl. Electrochem. 39 (2009) 1331–1337.
[11] F. Pico, E. Morales, J.A. Fernandez, T.A. Centeno, J. Ibañez, R.M. Rojas, J.M. Amarilla, J.M. Rojo, Electrochim. Acta 54 (2009) 2239–2245.
[12] F. Lufrano, P. Staiti, Energy Fuels 24 (2010) 3313–3320.
[13] Y. Zhang, Y.H. Gui, X.B. Wu, H. Feng, A.Q. Zhang, L.Z. Wang, T.C. Xia, Int. J. Hydrogen Energy 34 (2009) 2467–2470.
[14] J.W. Lang, L.B. Kong, M. Liu, Y.C. Luo, L. Kang, J. Electrochem. Soc. 157 (2010) A1341–A1346.
[15] Q.H. Huang, X.Y. Wang, J. Li, C.L. Dai, S. Gamboa, P.J. Sebastian, J. Power Sources 164 (2007) 425–429.
[16] G.H. Yuan, Z.H. Jiang, A. Aramata, Y.Z. Gao, Carbon 43 (2005) 2913–2917.
[17] J.Y. Lee, K. Liang, K.H. An, Y.H. Lee, Synth. Met. 150 (2005) 153–157.
[18] X.Y. Wang, X.Y. Wang, L. Liu, L. Bai, H.F. An, L.P. Zheng, L.H. Yi, J. Non Cryst. Solids 357 (2011) 793–797.
[19] X.Y. Wang, L. Liu, X.Y. Wang, L. Bai, H. Wu, X.Y. Zhang, L.H. Yi, Q.Q. Chen, J. Solid State Electrochem. 15 (2011) 643–648.
[20] H.Q. Wang, Z.S. Li, J. h. Yang, Q.Y. Li, X.X. Zhong, J. Power Sources 194 (2009) 1218–1221.
[21] H.C. Liang, F. Chen, R.G. Li, L. Wang, Z.H. Deng, Electrochim. Acta 49 (2004) 3463–3467.
[22] A. Jänes, H. Kurig, E. Lust, Carbon 45 (2007) 1226–1233.
[23] X.J. Zhang, W.H. Shi, J.X. Zhu, W.Y. Zhao, J. Ma, S. Mhaisalkar, T.L. Maria, Y.H. Yang, H. Zhang, H.H. Hng, Q.Y. Yan, Nano. Res. 3 (2010) 643–652.
[24] J.H. Kim, Y.S. Lee, A.K. Sharma, C.G. Liu, Electrochim. Acta 52 (2006) 1727–1732.
[25] A.B. Fuertes, F. Pico, J.M. Rojo, J. Power Sources 133 (2004) 329–336.
[26] D. Hulicova-Jurcakova, X. Li, Z.H. Zhu, R.D. Marco, G.Q. Lu, Energy Fuels 22 (2008) 4139–4145.
[27] A.G. Pandolfo, A.F. Hollenkamp, J. Power Sources 157 (2006) 11–27.
[28] C.Z. Yuan, X.G. Zhang, L.H. Su, B. Gao, L.F. Shen, J. Mater. Chem. 19 (2009) 5772–5777.